

Electronic and optical properties of graphene and graphitic ZnO nanocomposite structures

Wei Hu, Zhenyu Li, and Jinlong Yang^{a)}

Hefei National Laboratory for Physical Sciences at Microscale, and Department of Chemical Physics, University of Science and Technology of China, Hefei, Anhui 230026, People's Republic of China

(Received 15 January 2013; accepted 7 March 2013; published online 28 March 2013)

Electronic and optical properties of graphene and graphitic ZnO (G/g-ZnO) nanocomposites have been investigated with density functional theory. Graphene interacts overall weakly with g-ZnO monolayer via van der Waals interaction. There is no charge transfer between the graphene and g-ZnO monolayer, while a charge redistribution does happen within the graphene layer itself, forming well-defined electron-hole puddles. When Al or Li is doped in the g-ZnO monolayer, substantial electron (n-type) and hole (p-type) doping can be induced in graphene, leading to well-separated electron-hole pairs at their interfaces. Improved optical properties in graphene/g-ZnO nanocomposite systems are also observed, with potential photocatalytic and photovoltaic applications. © 2013 American Institute of Physics. [<http://dx.doi.org/10.1063/1.4796602>]

I. INTRODUCTION

Graphene, a two-dimensional (2D) sp^2 -hybridized carbon sheet, has received considerable interest recently owing to its intriguing properties.^{1–8} Graphene has a high carrier mobility, with a great potential for graphene-based electronic devices. Unfortunately, intrinsic electronic properties of graphene depend sensitively on the substrates, most of which tend to destroy the intrinsic electronic states of graphene and significantly lower its carrier mobility due to strong graphene-substrate interactions. Examples of such substrates include SiO_2 ,^{9–12} SiC,^{13–17} and some metal surfaces.^{18–21} Finding an ideal substrate for graphene remains a significant challenge.

Recently, several 2D graphene-based nanocomposites have been predicted theoretically and successfully synthesized in experiments, such as graphene/graphitic boron nitride (G/g-BN),^{22–24} graphene/MoS₂ nanosheet (G/MoS₂),^{25–27} graphene/MoSe₂ nanosheet (G/MoSe₂),^{28,29} and graphene/graphitic carbon nitride (G/g-C₃N₄).^{30,31} Importantly, most of them preserve intrinsic properties of graphene, especially, the high carrier mobility. Moreover, tunable band gaps can be opened at the Dirac point in these nanocomposites with a great potential for field effect transistors (FETs). Therefore, it would be very interesting to design and study new 2D graphene-based nanocomposites.

ZnO nanofilms and nanoparticles have been used with graphene as composite materials to obtain higher performance in applications, such as photovoltaic cells,^{32–37} supercapacitors,^{38,39} and FETs.⁴⁰ In fact, it is predicted by first-principles calculations^{41–44} and then confirmed experimentally⁴⁵ that ZnO(0001) film prefers a graphitic honeycomb structure when the layer number is reduced. 2D g-ZnO monolayer exhibits interesting electronic and magnetic properties.^{46–50} Therefore, besides commonly focused elec-

tronic structures, we expect more exciting new properties from a G/g-ZnO nanocomposite, such as optical properties.

At the same time, doping in the substrate materials of graphene based nanocomposites is a rarely studied topic. Impurities doped in ZnO nanomaterials, such as Al, Li, Cu, and N atoms substitutes, can significantly affect the properties of ZnO.^{51–53} Furthermore, impurities (Co, B, N, and C) have also been found to play an important role in g-ZnO monolayer.^{49,50} Therefore, different impurities doped in g-ZnO monolayer are also expected to induce electronic and optical property changes for G/g-ZnO nanocomposites.

In the present work, electronic structures and optical properties of G/g-ZnO nanocomposites have been investigated via first-principles calculations. Graphene is found to interact weakly with g-ZnO monolayer via weak van der Waals (vdW) interactions. Thus, intrinsic electronic properties of graphene, especially, high carrier mobility, can be preserved in G/g-ZnO nanocomposites. Electron-hole puddles on the graphene layer in G/g-ZnO nanocomposite are predicted, while well-separated electron and hole at the interfaces of G/doped g-ZnO nanocomposites are expected. Moreover, G/g-ZnO nanocomposites display different optical absorption compared to simplex graphene and g-ZnO monolayer.

II. THEORETICAL MODELS AND METHODS

The lattice parameters of graphene and g-ZnO monolayer calculated to setup unit cell are 2.47 and 3.29 Å, which fully agree with previous experimental measurements and theoretical studies.^{7,50} In order to simulate the G/g-ZnO nanocomposite, a 4×4 supercell of graphene (32 carbon atoms) is used to match a 3×3 supercell of g-ZnO monolayer (9 oxygen and 9 zinc atoms) with the lattice mismatch less than 1% (Fig. 1). Al and Li atoms substituted at Zn sites with a doping concentration of $1.2 \times 10^{14} \text{ cm}^{-2}$ are considered.

First-principles calculations are based on the density functional theory (DFT) implemented in the VASP package.⁵⁴

^{a)} Author to whom correspondence should be addressed. Electronic mail: jlyang@ustc.edu.cn

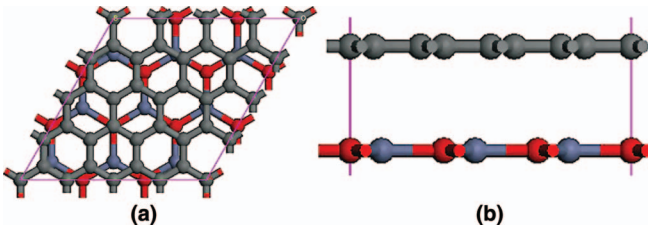


FIG. 1. Atomic structures of the G/g-ZnO nanocomposite ((a) top view and (b) side view). The gray, red, and blue balls denote carbon, oxygen, and zinc atoms, respectively.

The generalized gradient approximation of Perdew, Burke, and Ernzerhof (GGA-PBE)⁵⁵ with van der Waals correction proposed by Grimme (DFT-D2)⁵⁶ is chosen due to its good description of long-range vdW interactions.^{57–62} The energy cutoff is set to be 500 eV. The two-dimensional Brillouin zone is sampled with a 5×5 regular mesh and 480 k points are used for calculating the tiny band gaps at the Dirac point of graphene in the 4×4 supercell. The vacuum space in the Z direction is 15 Å to separate the interactions between neighboring slabs. All geometry structures were fully relaxed until the convergence criteria of energy and force are less than 10^{-5} eV and 0.01 eV/Å, respectively. Dipole correction is employed to cancel the errors of electrostatic potential, atomic force, and total energy, caused by periodic boundary condition.⁶³

To investigate the optical properties of G/g-ZnO nanocomposites, the frequency-dependent dielectric matrix is calculated.⁶⁴ The imaginary part of dielectric matrix is determined by a summation over states as

$$\varepsilon''_{\alpha\beta} = \frac{4\pi^2 e^2}{\Omega} \lim_{q \rightarrow 0} \frac{1}{q} \sum_{c,v,k} 2\omega_k \delta(\omega_{ck} - \omega_{vk} - \omega) \times \langle \mu_{ck+e_{aq}} | \mu_{vk} \rangle \langle \mu_{ck+e_{aq}} | \mu_{vk} \rangle^*, \quad (1)$$

where c and v represent the conduction and valence band states, respectively. μ_{ck} refers to the periodic part of the wavefunctions at the k point.

In order to evaluate the stability of hybrid G/g-ZnO nanocomposite, the interface binding energy is defined as

$$E_b = E_{G/g-ZnO} - E_{\text{Graphene}} - E_{g-ZnO}, \quad (2)$$

where $E_{G/g-ZnO}$, E_{Graphene} , and E_{g-ZnO} represent the total energy of G/g-ZnO nanocomposite, pristine graphene, and g-ZnO monolayer, respectively. As an benchmark, DFT-D2 calculations give a good bilayer distance of 3.25 Å and binding energy of -25 meV per carbon atom for bilayer graphene ($a = b = 2.47$ Å), which fully agree with previous experimental measurements^{65,66} and theoretical vdW calculations.⁶⁷

III. RESULTS AND DISCUSSION

Electronic properties of pristine graphene and g-ZnO monolayer are investigated first and their electronic band structures are plotted in Fig. 2. Monolayer graphene is a zero-gap semiconductor (Fig. 2(a)), showing a linear Dirac-like dispersion relation $E(k) = \pm \hbar v_F |k|$ around the Fermi energy, where v_F is the Fermi velocity and equal to 0.8×10^6 m/s in our band calculations, which agrees well with previous

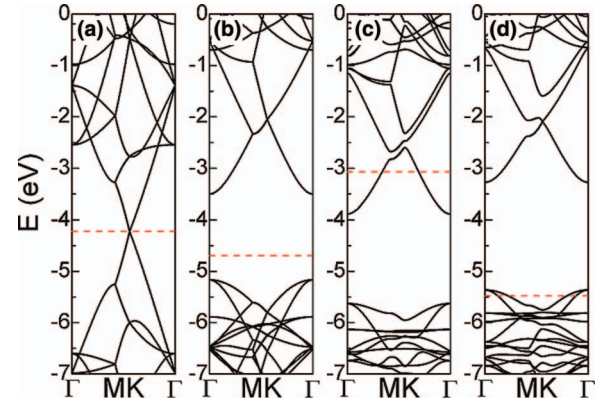


FIG. 2. Electronic band structures of (a) graphene, (b) g-ZnO, (c) Al, and (d) Li doped g-ZnO monolayers. The vacuum level is set to zero and the Fermi level is marked by red dotted lines.

theoretical studies,^{24,68} although DFT calculations underestimate the Fermi velocity of graphene by 15%–20%.⁶⁹ Monolayer g-ZnO is semiconducting with a direct band gap of 1.67 eV (Fig. 2(b)), which agrees well with previous theoretical studies,^{44,50} although GGA-PBE calculations always underestimate this value.⁷⁰ A calculation with screened hybrid HSE06 functional⁷¹ has given a band gap of 3.25 eV.⁵⁰ For doped g-ZnO monolayer (Figs. 2(c) and 2(d)), similar to other ZnO nanomaterials,⁵³ Al and Li atom substitutions induce n-type and p-type doping, respectively.

DFT-D2 calculated adsorption behaviors of G/g-ZnO nanocomposite systems are listed in Table I. A typical vdW equilibrium spacing of about 3.14 Å with a corresponding small binding energy of -51 meV per carbon atom are obtained for pristine g-ZnO monolayer, which are comparable with recent theoretical calculations in other 2D graphene-based nanocomposites, such as G/g-BN,^{22,24} G/MoS₂,²⁶ G/MoSe₂,²⁹ and G/g-C₃N₄.³¹ Even for doped g-ZnO monolayers, the interlayer distance and binding energy do not change much. Moreover, our DFT-D2 calculations on the G/g-ZnO nanocomposites are also fairly similar to recent more sophisticated calculations based on the random-phase approximation (RPA)^{72–74} for other graphene-substrate nanocomposites.^{75–79}

Electronic band structures of different G/g-ZnO nanocomposites are shown in Fig. 3. Only tiny band gaps of 5, 7, and 11 meV are opened at the Dirac point of graphene adsorption on pristine, Al and Li doped g-ZnO monolayers, respectively. Test calculations with a coarser k -point grid

TABLE I. DFT-D2 calculated equilibrium interfacial distance D_0 (Å), binding energy per carbon atom E_b (meV), graphene Dirac point shifts relative to the Fermi level ΔE_D (eV) in different G/g-ZnO nanocomposites, and the work function W_f (eV) of different g-ZnO monolayers. The work function of graphene is calculated to be $W_f = 4.3$ eV in this work. Previous theoretical results are 4.2–4.7 eV^{18,20} and experimental measurements are 4.6 eV.^{80,81}

DFT-D2	D_0	E_b	ΔE_D	W_f
Pristine	3.14	-51	0.00	...
Al doped	3.09	-62	-0.69	3.1
Li doped	3.16	-52	0.38	5.5

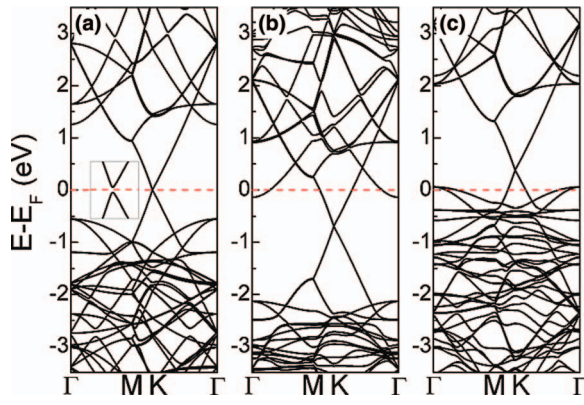


FIG. 3. Electronic band structures of (a) G/g-ZnO, (b) G/Al doped g-ZnO, and (c) G/Li doped g-ZnO nanocomposites. The Fermi level is set to zero and marked by red dotted lines.

indicate that hybrid HSE06 functional only slightly broaden the band gaps. These band gap values are significantly lower than thermal fluctuation (about 25 meV) at room temperature. Notice that induced graphene band gaps are typically sensitive to external conditions, such as interlayer separation,^{22,24} thus tunable, with potential applications for graphene-based FETs.

The Fermi level of G/g-ZnO nanocomposite remains in the induced gap, indicating that no charge transfer exists between graphene and undoped g-ZnO monolayer. This is also supported by their differential charge density ($\Delta\rho = \rho(\text{G/g-ZnO}) - \rho(\text{Graphene}) - \rho(\text{g-ZnO})$) plotted in Fig. 4(a). Notice that the inhomogeneous g-ZnO substrate induces charge redistribution in the graphene plane, forming intralayer electron-hole puddles,¹⁰ which may significantly enhance the electron conductivity and/or generate new photovoltaic and catalytic activities.³¹ Moreover, from electronic band calculations, the Fermi velocity at the Dirac point of graphene is almost unchanged ($v_F(\text{G/g-ZnO}) = 0.8 \times 10^6$ m/s) in G/g-ZnO nanocomposite compared to free-standing graphene.^{24,68} Therefore, pristine g-ZnO can be used as an ideal substrate for graphene with its electronic structures undisturbed.

Different charge rearrangement has been found in G/doped g-ZnO nanocomposites. Al and Li doped g-ZnO monolayers have a work function either 1.2 eV smaller or the same amount larger than that of pristine graphene as listed in Table I. Based on the Schottky-Mott model,⁸² the Dirac point of the composite systems is moved to below and above the Fermi level (Figs. 3(b) and 3(c)), respectively. As shown in

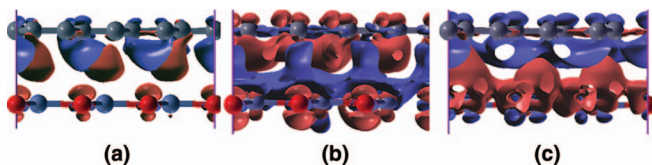


FIG. 4. Differential charge density with a isosurface value of $0.002 \text{ e}/\text{\AA}^3$ for (a) G/g-ZnO, (b) G/Al doped g-ZnO, and (c) G/Li doped g-ZnO nanocomposites. The red and blue regions indicate electron increase and decrease, respectively.

Figs. 4(b) and 4(c), electron-hole pairs are well separated at the interfaces of G/doped g-ZnO nanocomposites.

Based on the linear dispersion around the Dirac point of graphene,⁷ the charge carrier (electron or hole) concentration of doped graphene can be estimated by the following equation:^{83,84}

$$N_{e/h} = \frac{(\Delta E_D)^2}{\pi(\hbar v_F)^2}, \quad (3)$$

where ΔE_D is the Dirac point shift relative to the Fermi level. The calculated charge carrier density is $N_e(\text{G/n-type g-ZnO}) = 3.5 \times 10^{13} \text{ cm}^{-2}$ and $N_h(\text{G/p-type g-ZnO}) = 1.1 \times 10^{13} \text{ cm}^{-2}$. These values are remarkably close to the hole density ($3.0 \times 10^{13} \text{ cm}^{-2}$) of graphene on O-terminated TiO_2 surface⁸³ and more than 3 orders of magnitude larger than the intrinsic charge carrier concentration of graphene at room temperature ($n = \pi k_B^2 T^2 / 6 \hbar v_F^2 = 6 \times 10^{10} \text{ cm}^{-2}$).¹⁷ Compared to the charge carrier density of isolated Al and Li doped g-ZnO monolayers ($n = m\Delta E / \pi \hbar^2$, where ΔE is the difference between the Fermi level and conduction band minimum or valence band maximum),⁸⁵ the charge transfer efficiency is about 45% and 20%, respectively. Due to the underestimation of the band gap of g-ZnO monolayer, HSE06 calculations give even stronger charge transfer. Therefore, the charge transfer at the G/doped g-ZnO interfaces can induce effective electron and hole doping in graphene for graphene-based Schottky diodes⁸⁶⁻⁹³ and p-n junctions.^{94,95}

Finally, optical properties of G/g-ZnO nanocomposites are studied. Pristine graphene and g-ZnO monolayer themselves display unique optical properties.^{8,44} Interlayer interactions in G/g-ZnO nanocomposites may induce new optical transitions.^{31,96} Fig. 5 plots the imaginary part of dielectric functions for the light polarization perpendicular to the plane of graphene. Absorption edges should have a rigid shift (about 1.5 eV) due to the underestimation of the band gap in DFT calculations,⁷⁰ but it has been shown that the tendency of calculated optical properties in this way is reasonable.^{83,96,97} The

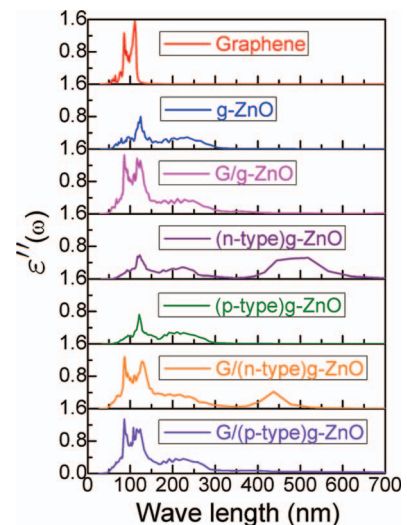


FIG. 5. Imaginary part (ϵ'') of dielectric function of graphene and g-ZnO monolayers as well as corresponding G/g-ZnO nanocomposites for the polarization vector perpendicular to the surface.

G/g-ZnO nanocomposite exhibits more effective UV absorption and enhanced visible light response, compared with g-ZnO monolayer. Redshift of the absorption edge is as large as 1.0 eV (100 nm) for G/g-ZnO nanocomposite, because electrons can now be directly excited from the valence band of graphene to the conduction band of g-ZnO monolayer.

Al doped n-type g-ZnO monolayer displays expanded optical absorption from UV into visible light and can harvest a broad range (400–600 nm) of visible light efficiently, while that is not found in Li doped p-type g-ZnO monolayer. For G/doped g-ZnO nanocomposites, the light absorption is much more complex. They still display much more effective UV absorption than doped g-ZnO monolayers. For G/n-type g-ZnO nanocomposite, there is an enhanced visible light response in the range of 300–400 nm but a small reduction in the range of 400–600 nm owing to part of electrons in n-type g-ZnO monolayer transfer into the graphene layer.

With the excellent electronic and optical properties combined, 2D G/g-ZnO nanocomposites are expected to be with a great potential in photocatalytic and photovoltaic applications.^{31,83,96} Electronically, the electron conductivity is enhanced, and also there are separating electrons and holes. Optically, UV and visible light adsorption is also enhanced compared to simplex graphene and g-ZnO monolayer.

IV. CONCLUSIONS

In summary, we have investigated electronic structures and optical properties of hybrid G/g-ZnO nanocomposites via first-principles calculations. Graphene is found to interact weakly with g-ZnO monolayer via weak vdW interactions. Electron-hole puddles are formed on the graphene layer in G/g-ZnO while they are well separated in G/doped g-ZnO nanocomposites. Substantial electron and hole doping in graphene on Al doped n-type and Li doped p-type g-ZnO monolayer, respectively, are induced by substrate. However, only tiny band gaps (meV) are opened at the Dirac point of graphene in all cases. High carrier mobility of graphene can be preserved in G/g-ZnO nanocomposites. Moreover, hybrid G/g-ZnO nanocomposites display enhanced and extended optical absorption compared to simplex graphene and g-ZnO monolayer.

ACKNOWLEDGMENTS

This work is partially supported by the National Key Basic Research Program (Grant No. 2011CB921404), by National Science Foundation of China (NSFC) (Grant Nos. 21121003, 91021004, 21233007, 20933006), by Chinese Academy of Sciences (CAS) (Grant No. XDB01020300), and by USTCSCC, SC-CAS, Tianjin, and Shanghai Supercomputer Centers.

¹K. S. Novoselov, A. K. Geim, S. V. Morozov, D. Jiang, M. I. Katsnelson, I. V. Grigorieva, S. V. Dubonos, and A. A. Firsov, *Nature (London)* **438**, 197 (2005).

²S. Y. Zhou, G.-H. Gweon, J. Graf, A. V. Fedorov, C. D. Spataru, R. D. Diehl, Y. Kopelevich, D.-H. Lee, S. G. Louie, and A. Lanzara, *Nat. Phys.* **2**, 595 (2006).

³T. Ohta, A. Bostwick, T. Seyller, K. Horn, and E. Rotenberg, *Science* **313**, 951 (2006).

⁴A. K. Geim and K. S. Novoselov, *Nat. Mater.* **6**, 183 (2007).

⁵J. C. Meyer, A. K. Geim, M. I. Katsnelson, K. S. Novoselov, T. J. Booth, and S. Roth, *Nature (London)* **446**, 60 (2007).

⁶A. K. Geim, *Science* **324**, 1530 (2009).

⁷A. H. C. Neto, F. Guinea, N. M. R. Peres, K. S. Novoselov, and A. K. Geim, *Rev. Mod. Phys.* **81**, 109 (2009).

⁸F. Bonaccorso, Z. Sun, T. Hasan, and A. C. Ferrari, *Nature Photon.* **4**, 611 (2010).

⁹M. Ishigami, J. H. Chen, W. G. Cullen, M. S. Fuhrer, and E. D. Williams, *Nano Lett.* **7**, 1643 (2007).

¹⁰J. Martin, N. Akerman, G. Ulbricht, T. Lohmann, J. H. Smet, K. von Klitzing, and A. Yacoby, *Nat. Phys.* **4**, 144 (2008).

¹¹P. Shemellaa and S. K. Nayak, *Appl. Phys. Lett.* **94**, 032101 (2009).

¹²N. T. Cuong, M. Otani, and S. Okada, *Phys. Rev. Lett.* **106**, 106801 (2011).

¹³S. Y. Zhou, G.-H. Gweon, A. V. Fedorov, P. N. First, W. A. de Heer, D.-H. Lee, F. Guinea, A. H. C. Neto, and A. Lanzara, *Nat. Mater.* **6**, 770 (2007).

¹⁴A. Mattausch and O. Pankratov, *Phys. Rev. Lett.* **99**, 076802 (2007).

¹⁵F. Varchon, R. Feng, J. Hass, X. Li, B. N. Nguyen, C. Naud, P. Mallet, J.-Y. Veuillen, C. Berger, E. H. Conrad, and L. Magaud, *Phys. Rev. Lett.* **99**, 126805 (2007).

¹⁶S. Kim, J. Ihm, H. J. Choi, and Y.-W. Son, *Phys. Rev. Lett.* **100**, 176802 (2008).

¹⁷J. Ristein, S. Mammadov, and T. Seyller, *Phys. Rev. Lett.* **108**, 246104 (2012).

¹⁸G. Giovannetti, P. A. Khomyakov, G. Brocks, V. M. Karpan, J. van den Brink, and P. J. Kelly, *Phys. Rev. Lett.* **101**, 026803 (2008).

¹⁹P. A. Khomyakov, G. Giovannetti, P. C. Rusu, G. Brocks, J. van den Brink, and P. J. Kelly, *Phys. Rev. B* **79**, 195425 (2009).

²⁰C. Gong, G. Lee, B. Shan, E. M. Vogel, R. M. Wallace, and K. Cho, *J. Appl. Phys.* **108**, 123711 (2010).

²¹M. Vanin, J. J. Mortensen, A. K. Kelkkanen, J. M. Garcia-Lastra, K. S. Thygesen, and K. W. Jacobsen, *Phys. Rev. B* **81**, 081408(R) (2010).

²²G. Giovannetti, P. A. Khomyakov, G. Brocks, P. J. Kelly, and J. van den Brink, *Phys. Rev. B* **76**, 073103 (2007).

²³C. R. Dean, A. F. Young, I. Meric, C. Lee, L. Wang, S. Sorgenfrei, K. Watanabe, T. Taniguchi, P. Kim, K. L. Shepard, and J. Hone, *Nature Nanotechnol.* **5**, 722 (2010).

²⁴Y. Fan, M. Zhao, Z. Wang, X. Zhang, and H. Zhang, *Appl. Phys. Lett.* **98**, 083103 (2011).

²⁵K. Chang and W. Chen, *Chem. Commun.* **47**, 4252 (2011).

²⁶Y. Ma, Y. Dai, M. Guo, C. Niu, and B. Huang, *Nanoscale* **3**, 3883 (2011).

²⁷L. Britnell, R. V. Gorbachev, R. Jalil, B. D. Belle, F. Schedin, A. Mishchenko, T. Georgiou, M. I. Katsnelson, L. Eaves, S. V. Morozov, N. M. R. Peres, J. Leist, A. K. Geim, K. S. Novoselov, and L. A. Ponomarenko, *Science* **335**, 947 (2012).

²⁸J. N. Coleman, M. Lotya, A. O'Neill, S. D. Bergin, P. J. King, U. Khan, K. Young, A. Gaucher, S. De, R. J. Smith, I. V. Shvets, S. K. Arora, G. Stanton, H.-Y. Kim, K. Lee, G. T. Kim, G. S. Duesberg, T. Hallam, J. J. Boland, J. Wang, J. F. Donegan, J. C. Grunlan, G. Moriarty, A. Shmeliov, R. J. Nicholls, J. M. Perkins, E. M. Grieveson, K. Theuwissen, D. W. McComb, P. D. Nellist, and V. Nicolosi, *Science* **331**, 568 (2011).

²⁹Y. Ma, Y. Dai, W. Wei, C. Niu, L. Yu, and B. Huang, *J. Phys. Chem. C* **115**, 20237 (2011).

³⁰Q. J. Xiang, J. G. Yu, and M. Jaroniec, *J. Phys. Chem. C* **115**, 7355 (2011).

³¹A. Du, S. Sanvito, Z. Li, D. Wang, Y. Jiao, T. Liao, Q. Sun, Y. H. Ng, Z. Zhu, R. Amal, and S. C. Smith, *J. Am. Chem. Soc.* **134**, 4393 (2012).

³²Y. J. Kim, J. H. Lee, and G. C. Yi, *Appl. Phys. Lett.* **95**, 213101 (2009).

³³J. Lin, M. Penchev, G. Wang, R. K. Paul, J. Zhong, X. Jing, M. Ozkan, and C. S. Ozkan, *Small* **6**, 2448 (2010).

³⁴S. W. Hwang, D. H. Shin, C. O. Kim, S. H. Hong, M. C. Kim, J. Kim, K. Y. Lim, S. Kim, S.-H. Choi, K. J. Ahn, G. Kim, S. H. Sim, and B. H. Hong, *Phys. Rev. Lett.* **105**, 127403 (2010).

³⁵X. Liu, L. Pan, T. Lv, T. Lu, G. Zhu, Z. Sun, and C. Sun, *Catal. Sci. Technol.* **1**, 1189 (2011).

³⁶H. Chang, Z. Sun, K. Y.-F. Ho, X. Tao, F. Yan, W.-M. Kwok, and Z. Zheng, *Nanoscale* **3**, 258 (2011).

³⁷T. Xu, L. Zhang, H. Cheng, and Y. Zhu, *Appl. Catal. B* **101**, 382 (2011).

³⁸Y. P. Zhang, H. B. Li, L. K. Pan, T. Lu, and Z. Sun, *J. Electroanal. Chem.* **634**, 68 (2009).

³⁹T. Lu, Y. Zhang, H. Li, L. Pan, Y. Li, and Z. Sun, *Electrochem. Acta* **55**, 4170 (2010).

- ⁴⁰Y. Y. Hui, G. Tai, Z. Sun, Z. Xu, N. Wang, F. Yan, and S. P. Lau, *Nanoscale* **4**, 3118 (2012).
- ⁴¹F. Claeysens, C. L. Freeman, N. L. Allan, Y. Sun, M. N. R. Ashfold, and J. H. Harding, *J. Mater. Chem.* **15**, 139 (2005).
- ⁴²C. L. Freeman, F. Claeysens, and N. L. Allan, *Phys. Rev. Lett.* **96**, 066102 (2006).
- ⁴³Z. C. Tu and X. Hu, *Phys. Rev. B* **74**, 035434 (2006).
- ⁴⁴Z. C. Tu, *J. Comput. Theor. Nanosci.* **7**, 1182 (2010).
- ⁴⁵C. Tusche, H. L. Meyerheim, and J. Kirschner, *Phys. Rev. Lett.* **99**, 026102 (2007).
- ⁴⁶M. H. Wu, X. J. Wu, Y. Pei, and X. C. Zeng, *Nano Res.* **4**, 233 (2011).
- ⁴⁷E. J. Kan, H. J. Xiang, F. Wu, C. Tian, C. Lee, J. L. Yang, and M.-H. Whangbo, *Appl. Phys. Lett.* **97**, 122503 (2010).
- ⁴⁸Y. Wang, Y. Ding, J. Ni, S. Shi, C. Li, and J. Shi, *Appl. Phys. Lett.* **96**, 213117 (2010).
- ⁴⁹T. M. Schmidt, R. H. Miwa, and A. Fazzio, *Phys. Rev. B* **81**, 195413 (2010).
- ⁵⁰H. Guo, Y. Zhao, N. Lu, E. Kan, X. C. Zeng, X. Wu, and J. Yang, *J. Phys. Chem. C* **116**, 11336 (2012).
- ⁵¹M. Venkatesan, C. B. Fitzgerald, J. G. Lunney, and J. M. D. Coey, *Phys. Rev. Lett.* **93**, 177206 (2004).
- ⁵²L.-H. Ye, A. J. Freeman, and B. Delley, *Phys. Rev. B* **73**, 033203 (2006).
- ⁵³A. A. Sokol, S. A. French, S. T. Bromley, C. R. A. Catlow, H. J. J. van Dame, and P. Sherwoode, *Faraday Discuss.* **134**, 267 (2007).
- ⁵⁴G. Kresse and J. Hafner, *Phys. Rev. B* **47**, 558 (1993).
- ⁵⁵J. P. Perdew, K. Burke, and M. Ernzerhof, *Phys. Rev. Lett.* **77**, 3865 (1996).
- ⁵⁶S. Grimme, *J. Comput. Chem.* **27**, 1787 (2006).
- ⁵⁷S. Grimme, C. Muck-Lichtenfeld, and J. Antony, *J. Phys. Chem. C* **111**, 11199 (2007).
- ⁵⁸J. Antony and S. Grimme, *Phys. Chem. Chem. Phys.* **10**, 2722 (2008).
- ⁵⁹T. Bucko, J. Hafner, S. Lebegueand, and J. G. Angyan, *J. Phys. Chem. A* **114**, 11814 (2010).
- ⁶⁰R. Kagimura, M. S. C. Mazzoni, and H. Chacham, *Phys. Rev. B* **85**, 125415 (2012).
- ⁶¹L. Yuan, Z. Li, J. Yang, and J. G. Hou, *Phys. Chem. Chem. Phys.* **14**, 8179 (2012).
- ⁶²Y. Ma, Y. Dai, M. Guo, and B. Huang, *Phys. Rev. B* **85**, 235448 (2012).
- ⁶³G. Makov and M. C. Payne, *Phys. Rev. B* **51**, 4014 (1995).
- ⁶⁴M. Gajdoš, K. Hummer, and G. Kresse, *Phys. Rev. B* **73**, 045112 (2006).
- ⁶⁵Y. Baskin and L. Mayer, *Phys. Rev.* **100**, 544 (1955).
- ⁶⁶R. Zacharia, H. Ulbricht, and T. Hertel, *Phys. Rev. B* **69**, 155406 (2004).
- ⁶⁷R. E. Mapasha, A. M. Ukpong, and N. Chetty, *Phys. Rev. B* **85**, 205402 (2012).
- ⁶⁸R. Qin, C.-H. Wang, W. Zhu, and Y. Zhang, *AIP Adv.* **2**, 022159 (2012).
- ⁶⁹M. Calandra and F. Mauri, *Phys. Rev. B* **76**, 205411 (2007).
- ⁷⁰S. Lany and A. Zunger, *Phys. Rev. B* **78**, 235104 (2008).
- ⁷¹J. Heyd, G. E. Scuseria, and M. Ernzerhof, *J. Chem. Phys.* **124**, 219906 (2006).
- ⁷²J. Harl and G. Kresse, *Phys. Rev. B* **77**, 045136 (2008).
- ⁷³J. Harl and G. Kresse, *Phys. Rev. Lett.* **103**, 056401 (2009).
- ⁷⁴J. Harl, L. Schimka, and G. Kresse, *Phys. Rev. B* **81**, 115126 (2010).
- ⁷⁵S. Lebègue, J. Harl, T. Gould, J. G. Ángyán, G. Kresse, and J. F. Dobson, *Phys. Rev. Lett.* **105**, 196401 (2010).
- ⁷⁶B. Sachs, T. O. Wehling, M. I. Katsnelson, and A. I. Lichtenstein, *Phys. Rev. B* **84**, 195414 (2011).
- ⁷⁷T. Olsen, J. Yan, J. J. Mortensen, and K. S. Thygesen, *Phys. Rev. Lett.* **107**, 156401 (2011).
- ⁷⁸T. Björkman, A. Gulans, A. V. Krasheninnikov, and R. M. Nieminen, *Phys. Rev. Lett.* **108**, 235502 (2012).
- ⁷⁹T. Björkman, A. Gulans, A. V. Krasheninnikov, and R. M. Nieminen, *J. Phys.: Condens. Matter* **24**, 424218 (2012).
- ⁸⁰Y. J. Yu, Y. Zhao, S. Ryu, L. E. Brus, K. S. Kim, and P. Kim, *Nano Lett.* **9**, 3430 (2009).
- ⁸¹S. J. Sque, R. Jones, and P. R. Briddon, *Phys. Status Solidi A* **204**, 3078 (2007).
- ⁸²J. Bardeen, *Phys. Rev.* **71**, 717 (1947).
- ⁸³A. Du, Y. H. Ng, N. J. Bell, Z. Zhu, R. Amal, and S. C. Smith, *J. Phys. Chem. Lett.* **2**, 894 (2011).
- ⁸⁴Z. Chen, I. Santoso, R. Wang, L. F. Xie, H. Y. Mao, H. Huang, Y. Z. Wang, X. Y. Gao, Z. K. Chen, D. Ma, A. T. S. Wee, and W. Chen, *Appl. Phys. Lett.* **96**, 213104 (2010).
- ⁸⁵Y. Zhang and J. Singh, *J. Appl. Phys.* **85**, 587 (1999).
- ⁸⁶X. Wu, M. Sprinkle, X. Li, F. Ming, C. Berger, and W. A. de Heer, *Phys. Rev. Lett.* **101**, 026801 (2008).
- ⁸⁷Y. Yoon, G. Fiori, S. Hong, G. Iannaccone, and J. Guo, *IEEE Trans. Electron Devices* **55**, 2314 (2008).
- ⁸⁸D. Jimenez, *Nanotechnology* **19**, 345204 (2008).
- ⁸⁹S. Tongay, T. Schumann, and A. F. Hebard, *Appl. Phys. Lett.* **95**, 222103 (2009).
- ⁹⁰X. Li, H. Zhu, K. Wang, A. Cao, J. Wei, C. Li, Y. Jia, Z. Li, Xi. Li, and D. Wu, *Adv. Mater.* **22**, 2743 (2010).
- ⁹¹S. Tongay, T. Schumann, X. Miao, B. R. Appleton, and A. F. Hebard, *Carbon* **49**, 2033 (2011).
- ⁹²C.-C. Chen, M. Aykol, C.-C. Chang, A. F. J. Levi, and S. B. Cronin, *Nano Lett.* **11**, 1863 (2011).
- ⁹³H. Yang, J. Heo, S. Park, H. J. Song, D. H. Seo, K.-E. Byun, P. Kim, I. K. Yoo, H.-J. Chung, and K. Kim, *Science* **336**, 1140 (2012).
- ⁹⁴H. Sojoudi, J. Baltazar, L. M. Tolbert, C. L. Henderson, and S. Graham, *Appl. Mater. Interfaces* **4**, 4781 (2012).
- ⁹⁵J. Baltazar, H. Sojoudi, S. A. Paniagua, J. Kowalik, S. R. Marder, L. M. Tolbert, S. Graham, and C. L. Henderson, *J. Phys. Chem. C* **116**, 19095 (2012).
- ⁹⁶F. Wu, Y. Liu, G. Yu, D. Shen, Y. Wang, and E. Kan, *J. Phys. Chem. Lett.* **3**, 3330 (2012).
- ⁹⁷J. Yang, Y. Zhai, H. Liu, H. Xiang, X. Gong, and S. Wei, *J. Am. Chem. Soc.* **134**, 12653 (2012).